

DLR HABLEG – HIGH ALTITUDE BALLOON LAUNCHED EXPERIMENTAL GLIDER

Sven Wlach⁽¹⁾, Marc Schwarzbach⁽²⁾, Maximilian Laiacker⁽³⁾

⁽¹⁾DLR - Institute of Robotics and Mechatronics, Oberpfaffenhoffen, Germany, sven.wlach@dlr.de

⁽²⁾DLR - Institute of Robotics and Mechatronics, Oberpfaffenhoffen, Germany, marc.schwarzbach@dlr.de

⁽³⁾DLR - Institute of Robotics and Mechatronics, Oberpfaffenhoffen, Germany, maximilian.laiacker@dlr.de

NOMENCLATURE

DLR	German Aerospace Center
ELHASPA	Electric High Altitude Solar Powered Aircraft
HABLEG	High Altitude Balloon Launched Experimental Glider
HAPS	High Altitude Pseudo-Satellite
IMU	Inertial Measurement Unit
RF	Radio Frequency
UAV	Unmanned Aerial Vehicle
VEXREDUS	Vehicle with Extended Reentry Duration - University of Stuttgart

ABSTRACT

The group *Flying Robots* at the *DLR Institute of Robotics and Mechatronics* in Oberpfaffenhofen conducts research on solar powered high altitude aircrafts. Due to the high altitude and the almost infinite mission duration, these platforms are also denoted as High Altitude Pseudo-Satellites (HAPS).

This paper highlights some aspects of the design, building, integration and testing of a flying experimental platform for high altitudes. This unmanned aircraft, with a wingspan of 3 m and a mass of less than 10 kg, is meant to be launched as a glider from a high altitude balloon in 20 km altitude and shall investigate technologies for future large HAPS platforms.

The aerodynamic requirements for high altitude flight included the development of a launch method allowing for a safe transition to horizontal flight from free-fall with low control authority.

Due to the harsh environmental conditions in the stratosphere, the integration of electronic components in the airframe is a major effort.

For regulatory reasons a reliable and situation dependent flight termination system had to be implemented.

In May 2015 a flight campaign was conducted. The mission was a full success demonstrating that stratospheric research flights are feasible with rather small aircrafts.

1. INTRODUCTION

High Altitude Pseudo-Satellites (HAPS) are platforms

capable of flying well above the weather and common air traffic for a prolonged or almost indefinite time. In a typical mission scenario a HAPS loiters above a targeted region providing satellite-like ground coverage from its stratospheric flight altitude. However, except from a handful research and development vehicles no actual operational vehicle exists to date. Potential applications are plentiful ranging from earth observation, disaster support, cellular network and Internet coverage over security services to stratospheric or general scientific research. Compared to satellites, these platforms would have the major advantage of a quick deployment and replacement. Yet, to achieve continuous stratospheric flight, new technologies have to be developed.

The German Aerospace Center DLR has been conducting research in this field over the past few years, by studying the feasibility of solar powered high altitude aircrafts. Associated with this effort was the construction of ELHASPA in collaboration with several companies of the aerospace industry. ELHASPA, an abbreviation for Electric High Altitude Solar Powered Aircraft, was used for the research and demonstration of key technologies needed for this kind of platforms

Due to a student project (VEXREDUS), the author of this paper already gathered some experience in this field by launching unmanned aircrafts from high altitude balloons. This led to the idea to test technologies for future HAPS platforms by building a rather compact aircraft in the sub-10 kg range, launch it from a balloon in 20 km altitude and let it autonomously return to the base. This High Altitude Balloon Launched Experimental Glider (HABLEG) would thereby offer valuable testing time in the stratospheric environment encountered by HAPS at moderate costs.

The goals of this experiment are:

- Gaining operational experience regarding high-altitude and beyond-visual-range missions with reduced safety concerns and financial risk
- Testing of existing and new hardware in the HAPS flight regime
- Testing of HAPS flight software
- Testing of additional scientific payload (optional)

The envisioned mission for HABLEG consists of the following phases, as also illustrated in Figure 1:

- Ascent on balloon
- Launch and drop
- Transition to horizontal flight
- High altitude flight experiments
- Return to Land
- Landing

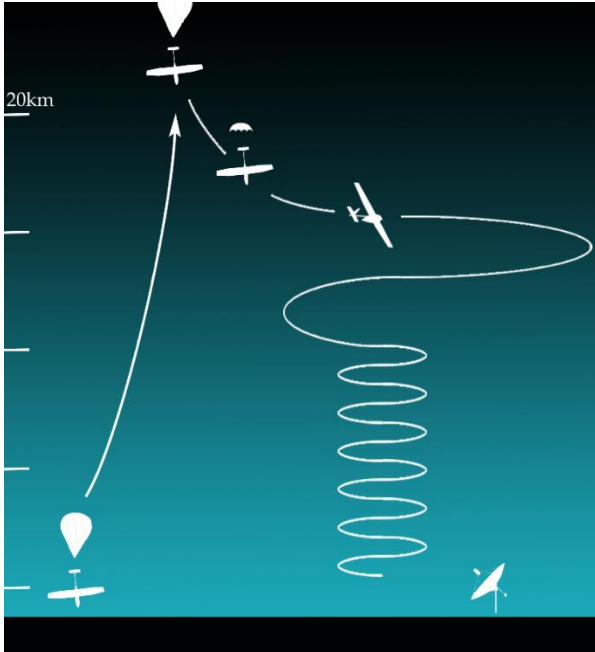


Figure 1: HABLEG flight phases

2. SYSTEM OVERVIEW

The aircraft, as pictured in Figure 2, has a wingspan of 3m and weighs 7.4 kg.



Figure 2: HABLEG next to antenna tracker

The general design idea was to have a large central avionic box containing all major flight electronics, which can be taken out easily for testing. Its form factor is close to a format that would be suitable for larger platforms. Furthermore, the wish for a large payload bay close to the plane's center of gravity existed, in order to fly experiments in the future.

Figure 3 shows a side view of the fuselage. It contains a camera bay (1) in the nose, a battery bay (2) and an avionics bay (3), which houses the already mentioned avionics box. This is followed by the roughly shoe carton sized payload bay (4) and an aft located parachute bay (5) accommodating the flight termination system.

The wing features special low Reynold number airfoils to allow for a stable high altitude flight at moderate speeds. This is especially important during the launch from the balloon and transition to horizontal flight, which is the most critical part of the mission.

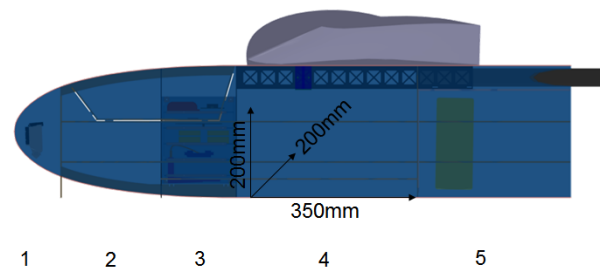


Figure 3: HABLEG Fuselage: (1) camera bay, (2) battery bay, (3) avionics bay, (4) payload bay, (5) parachute bay

The system uses two RF-links on 2.4 GHz and 868 MHz for two-way data communication, as well as a 2.3 GHz analogue video downlink. Data is received and transmitted with the antenna tracking system also shown in Figure 2, whereas the video is received by a separate 2.5 m diameter parabolic antenna.

In total, the aircraft carries four cameras, three of them for flight documentation and one for live video.

As a first hardware experiment, DLR in-house developed actuators, were flown on the mission, controlling elevator and rudder. Those actuators, pictured in

Figure 4, use harmonic drives as gear technology and are derived from robotic drives used widely in the institute's robotic systems.

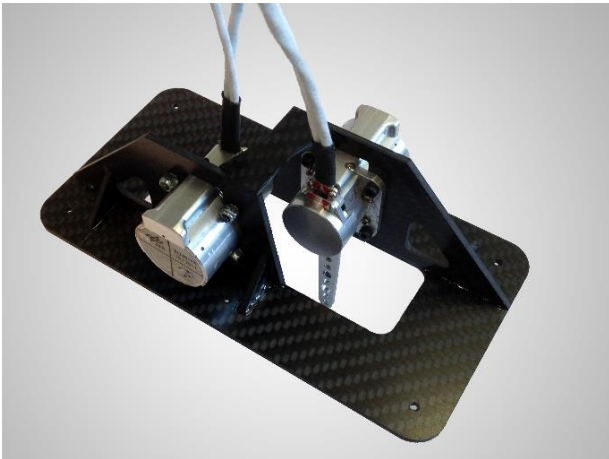


Figure 4: DLR harmonic drive actuators

3. LAUNCH METHOD

Aerodynamic design is a major concern for stratospheric flight. Driving factors for the experiment were good stall stability and recoverability, which is a combined design process of airfoil choice and wing planform definition. Further constraints are found in structural stability, buildability, weight and transportability, which all mainly affect the possible wingspan. The greatest challenge, however, consists in launching the plane from the balloon, as pictured in Figure 5.

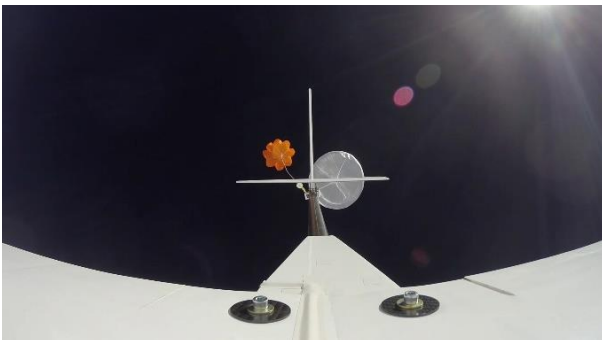


Figure 5: HABLEG shortly after release from balloon. The drogue chute is used for stabilisation during the initial drop phase, to prevent the glider from entering an unescapable flat spin.

As a result of the low density atmosphere, the aircraft needs to fall for a period of time to reach a speed at which flying is possible. During this drop phase, it is possible that an initial rotation is not dampened due to the low effectiveness of the horizontal and vertical stabilizer in that situation. This might lead to an unescapable flat spin. In fact, prior projects revealed that this is even more problematic than one might think initially. The VEXREDUS project, [1] showed that since the plane is still ascending on the balloon upon

release, the inertia carries it a few meters further upwards. Due to the reverse air flow, the originally nose-down oriented aircraft pitches up so that it ends in an almost horizontal attitude with zero speed. At these altitudes a conventional aircraft configuration, as it is the case with HABLEG, is then very likely to enter a tail spin or flat spin. The aircraft needs to fly around 45 m/s to achieve level flight at an altitude of 20 km. In order to reach this velocity safely, the plane needs to be stabilized during the drop phase. It was decided to realize this with a small drogue chute attached at the end of the tail boom that can be released on command. The launch sequence is implemented like this:

- During ascent the glider is suspended on a main rope running from the balloon, through a rope guide at the very end of the tail boom to a clutch located near the elevator. The drogue chute and its rope are stowed in a jar attached to the main rope close to the aircraft. The drogue chute rope also runs through a guide to a second clutch. All the control surfaces are set to neutral position prior to launch.
- When the launch command is given, the primary clutch releases the main rope to the balloon.
- While the glider pitches nose upwards, the balloon continues to ascent and thereby pulls the drogue out of the jar.
- The aircraft now starts free-falling, with a probably unsuitable orientation. With increasing vertical speed, the drogue chute starts to develop drag and pulls on the tail of the aircraft, which is thereby aligned nose downwards, as in Figure 5.
- After a fixed time the autopilot is set to dampen roll and pitch motions.
- By either reaching a predefined speed or a set time limit the second clutch is actuated to release the drogue chute.
- The autopilot now gently starts to pull out the glider while keeping the wings leveled.
- After reaching a preset pitch angle or a time limit, the autopilot changes the flight mode to return home.

4. THERMAL ASPECTS OF SYSTEM INTEGRATION

Due to the harsh environmental conditions encountered during stratospheric flight, thermal suitability had to be considered during system integration. For example, the long rudder linkages to the tail planes were implemented as carbon push-pull rods, which is the same material as the tail boom. Calculations showed,

that the use of steel-wire pull chords would probably destroy the control surface, due to the enormous forces resulting from different thermal expansion coefficients.

The overall thermal concept has different zones of thermal requirements. The fuselage is lined with Styrofoam on the inside, which provides basic insulation against the cold environment, as it can be seen in Figure 6.



Figure 6: Battery and avionics bay with insulation. The avionics box is secured in place by a snap-in mechanism and is thereby easily removable for testing.

Regarding temperatures, IMU and batteries are the most critical components. Figure 7 shows how the IMU is located within the avionics box on the top layer, where several heat-producing components provide a mild operating environment.

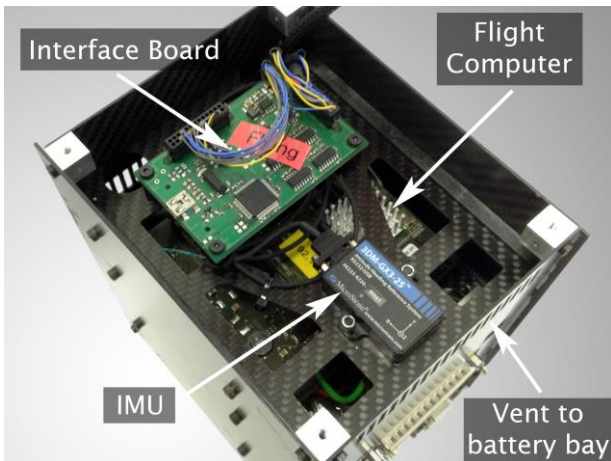


Figure 7: Avionics box with top cover removed. The IMU is located over heat producing components such as flight control computer, servo motor controllers and primary radio modem. The open carbon structure allows for air circulation

The excess heat mostly vents to the front into the battery

bay. Since the battery cells produce only very little heat by themselves at the occurring small currents, this, together with some additional insulation, is vital to obtain the batteries rated performance.

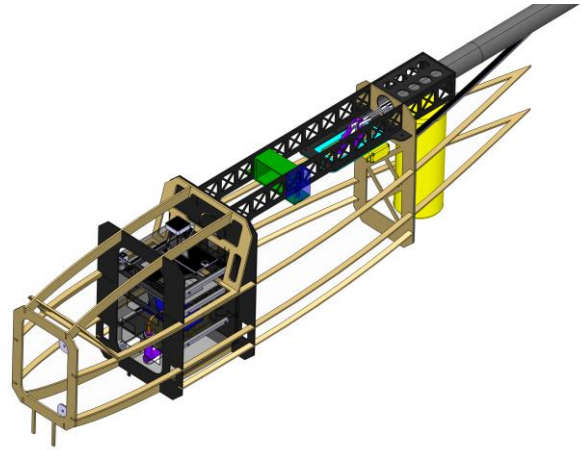


Figure 8: Inner fuselage structure. The avionics box mostly vents the excess heat to the front into the battery bay

The payload bay is insulated but sees colder temperatures due to venting through the open tail boom. The parachute bay isn't insulated at all.

Some components like video transmitter, secondary data modem and aileron servos are integrated into the wings foam core and are thereby only slightly insulated.

The system has no need for active thermal control elements like heaters or controllable air inlets.

The concept was tested in a thermal-vacuum chamber at the Institute of Space Systems of the University of Stuttgart. The chamber is meant for subsystem tests of satellite components, thereby only offering an interface temperature over a bottom-located cooling plate. To distribute the coldness, the fuselage was placed within an insulated box that sat on top of the cooling plate, as pictured in Figure 9. Using fans blowing on the cooling plate, some airflow could be simulated.

Figure 10 plots the temperatures over time during the test. For the test the pressure was slowly lowered to about 60 mbar over a time span of 10 min. This corresponds to an ISA altitude of 19 to 20 km. Cooling was initiated only after reaching the low pressure state to prevent the formation of ice on the cooling plate. In general, all the systems performed well. The temperatures in the avionics box showed a maximum of 38°C at the IMU and 66°C at the CPU (not in diagram), which is relatively warm, but not critical. Since the outside temperature in the insulation box was only able to reach -16°C, due to the limited cooling capacity of

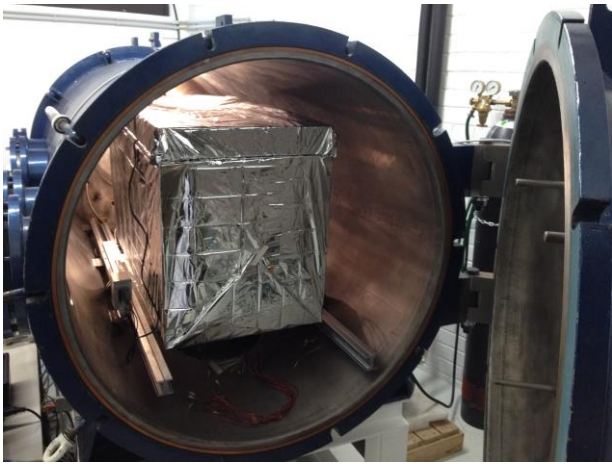


Figure 9: Insulation box inside the thermal vacuum chamber

the bottom-plate, this combination of low density and relatively “warm” surrounding air is a worst-case scenario regarding overheating.

An interesting behavior was discovered in the curve of one of the 12V DC/DC converters, located on the power supply board inside the avionics box. Here, at some point a spike in the temperature profile appears and reappears after some time. The sudden increase in temperature points to a significantly risen demand on this power rail. The periodicity suggested that it was a controlled event. After some investigation, the source

was found within the airdata measurement electronics, which have an integrated heating element that activates as temperatures drop. Since the model was originally believed to be without a heater and the current drawn was on a critical level for the DC/DC converter, the equipment was later swapped for a model without heating. As already mentioned, another focus was the temperature development of the video transmitter. A first result was that at sea level conditions and without air flow over the heat sink, the transmitter heats up to almost 60°C, which is hotter than the operating limit of 55°C. Therefore, it was decided to use an external fan during longer periods of ground handling. Subsequently it also became clear during chamber testing that a low pressure environment without air flow would lead to an overheating of the device. On the other hand, turning on the fan facing the cooling plate resulted in a major temperature drop, since the resulting airflow passed by the device. While the transmitter itself is located inside the foam core of the wing, its heat sink sticks out of the surface and is thereby directly subjected to the cold environment, as pictured in Figure 11. The large temperature drop, as consequence of enforced convection, led to adding a flow shield in front of the heat sink in flight direction. This has almost no effect during the low speed ascent, but creates a wake of low speed reversed flow at the heat sink during the flight. By this measure the heat sink can divert enough heat during the low speed ascent, but will not cool the transmitter below a critical level during the flight.

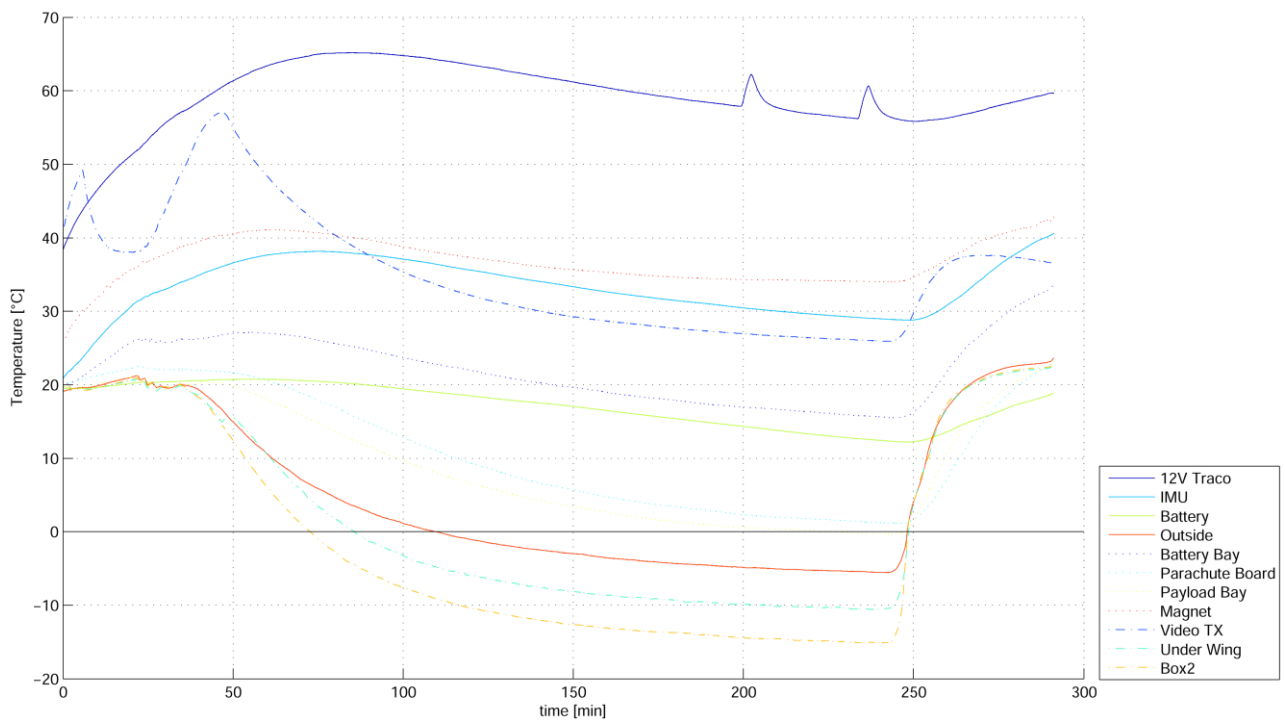


Figure 10: Temperature development during thermal vacuum chamber test



Figure 11: Video transmitter with heatsink on the lower side of the wing

5. FLIGHT TERMINATION SYSTEM

Though the flight test zone is located in a very remote place, the flight has to be conducted in a specific area. The main concern is a fly-away of the vehicle, which can travel great distances from the planned mission altitude. Therefore, a reliable flight termination system had to be implemented, that reduces the possible range, as well as the impact energy to a level, where it poses no significant threat to humans, as demanded by the ESRANGE Safety Manual [2].

The system uses two different flight termination modes. One is temporary using control surface deflection to put the aircraft into a recoverable tail spin. The other is permanent by deploying a parachute that allows the rescue of the whole system in case of a failure. The parachute hatch is kept closed by an electromagnet, so even in the case of total power loss, the chute is ejected.

Figure 12 shows the inside of the parachute bay. The parachute (5) is folded inside a plastic container (4). The container is cut open, thereby holding the parachute in place while still allowing it to be pulled out easily. The parachute is attached to the parachute bays hood with a rope. This hood is spring-loaded (2) and kept in place by several guides (3, 6, 7, 8, 10, 11) and an electromagnet (1). This magnet is controlled by a separate and simple micro-controller which receives a live or release signal from a central interface board monitoring the flight computer health and also enables the direct pass-through of tele commands. If the pulsing live signal from this interface board stops or a release signal is received, the magnet is deactivated. A power loss of the system would as well affect the magnet. Therefore, both cases lead to the hood being jettisoned by the spring, which then pulls out the parachute. The concept required a clean alignment of all the guiding parts as well as the magnet and its metal counter plate

(9), to ensure a reliable jettison of the hood, while still securing it safely under all the aerodynamic loads during normal operation.

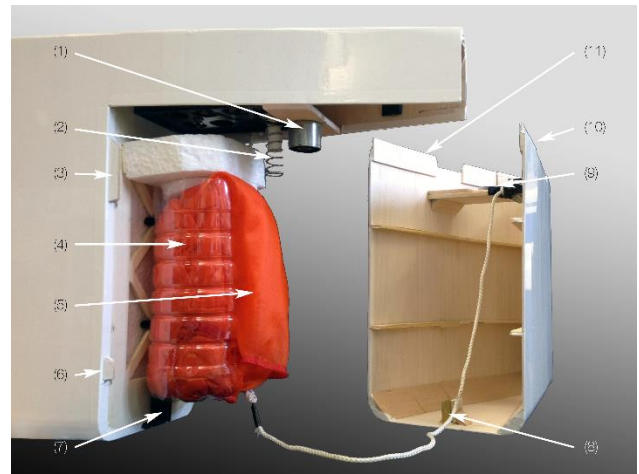


Figure 12: Flight Termination System: The aft section of the fuselage is spring-loaded. An electromagnet keeps it attached during normal operation

The maximum opening force is the highest occurring force produced by the parachute during the opening process. Since this force is exerted over the parachute rope on the aircraft's structure, it is important to know its magnitude. It was calculated according to Knacke, [3] (p. 5-50). Figure 13 plots the maximum opening force in different altitudes at various speeds. The magenta colored lines show the isobars of dynamic pressure. In normal operation an airspeed corresponding to the dynamic pressure of 30 m/s at sea level conditions should not be exceeded. This is highlighted by the thicker solid isobar. The rope and its attachment are dimensioned to hold at least 350 N, corresponding to 50 m/s at sea level conditions.

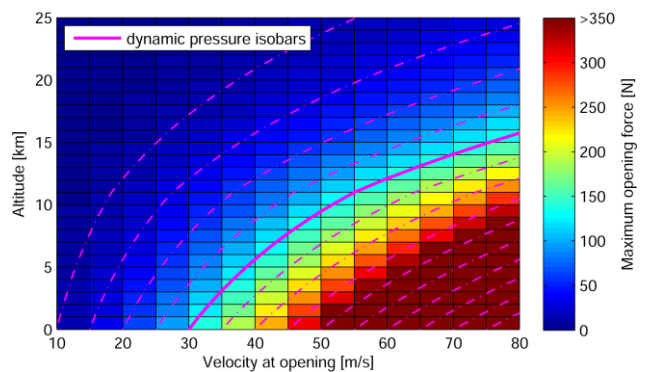


Figure 13: Maximum parachute opening force at different speeds and altitudes

6. FLIGHT CAMPAIGN

The flight campaign was conducted in May 2015 at the rocket base ESRANGE in northern Sweden. Regarding weather, there were several constraints, the most prominent being the wind direction. Since the allowed test area for UAVs is V-shaped and opening to the north, as marked in Figure 14 by the red surrounding area, south wind was needed to drift into this section. Furthermore, the overall wind velocity must be low enough to not exceed the range limit of the radio link during ascent. Heavy rain at base would also adversely affect the radio links performance.

Only a few days after arrival, on Friday the 8th, weather conditions were favorable and the mission was launched.

The ascent, colored magenta in Figure 14, took 77 min. At 19550m altitude and 66km ground distance the release command was given. After falling for several seconds and adjusting control parameters of the attitude control loops, stable flight was achieved in about 18100m altitude followed by a coordinated turn towards base.

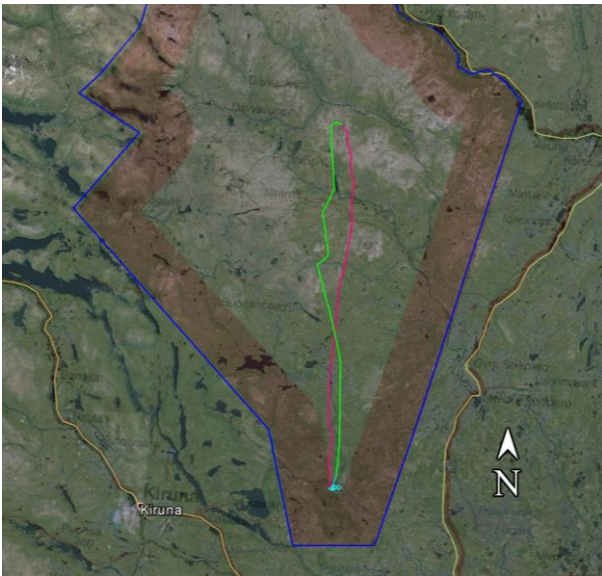


Figure 14: Flightpath and flight-test area

Figure 15 depicts the view over the left wing as it presented itself right after the turn to base had been completed.



Figure 15: Stable stratospheric flight

From release to landing the flight lasted 68min. During the flight home, marked in green, course changes were commanded to test the navigational behavior. Also, experiments regarding different flight path angles and flight speeds were conducted, to optimize the headwind performance in different altitudes. Figure 16 is taken from the front facing camera while flying towards the landing site.



Figure 16: View of front-facing camera during cruise flight towards home base

The aircraft arrived in about 4500m altitude at the landing site from where it was commanded into different flying patterns until finally, 200m above ground, the planned switch to manual control occurred, to allow for a more defined landing in an area of several obstacles. After a total mission time of 145min touchdown occurred just 80m away from the launch site. At that point the aircraft had travelled an overall distance of 169km.



Figure 17: HABLEG during final approach for landing

7. CONCLUSION

The success of the HABLEG mission demonstrated that stratospheric research flights are feasible with relatively small platforms.

Future work will focus on how balloon launched planes can complement the research and development of stratospheric solar platforms.

Furthermore, there are also many opportunities for further developments and applications directly using small scale platforms to conduct scientific experiments. Therefore, the goal is to also extend the capabilities of these smaller aircrafts regarding altitude, flight time and launch convenience.

8. References

[1] D. Steenari, T. Kuhn and S. Wlach: VEXREDUS: A Student High Altitude Glider Project to Demonstrate the Capabilities of a Blended Wing Body Concept. In: Proc. '21st ESA Symposium on European Rocket & Balloon Programmes and Related Research', Thun, Switzerland (ESA SP-721, October 2013).

[2] <http://www.sscspace.com/file/esrange-safety-manual.pdf> - ESRANGE Safety Manual

[3] T. W. Knacke: Parachute Recovery Systems - Design Manual. Para Publ., 1992, ISBN-13: 978-0915516858.